Geology, Geophysics & Environment 2021, vol. 47 (3): 143–157

Sulfur and lead isotope geochemical characteristics of Pb-Zn deposits in the Khau Loc zone, northeastern Vietnam, and their significance

Khuong The Hung[1], Ta Dinh Tung[2], Do Quoc Binh[3], Pham Nhu Sang[4], Nguyen Thi Cuc[5], Nguyen Thi Hoang Linh[6], Quach Duc Tin[7]

[1] Hanoi University of Mining and Geology; 100000 Hanoi, Vietnam; e-mail: khuongthehung@humg.edu.vn (corresponding author); ORCID ID: 0000-0003-1544-6470
[2] Vietnam Institute of Geosciences and Mineral Resources; 100000 Hanoi, Vietnam; e-mail: tadinhtung1985@gmail.com
[3] Vietnam Institute of Geosciences and Mineral Resources; 100000 Hanoi, Vietnam; e-mail: binhdq2004@gmail.com
[4] Hanoi University of Mining and Geology; 100000 Hanoi, Vietnam; e-mail: phamnhusang@humg.edu.vn); ORCID ID: 0000-0002-5557-7419
[5] Hanoi University of Mining and Geology; 100000 Hanoi, Vietnam; e-mail: nguyenthicuc@humg.edu.vn
[6] Vietnam Institute of Geosciences and Mineral Resources; 100000 Hanoi, Vietnam; e-mail: nthlinh80@gmail.com
[7] Vietnam Institute of Geosciences and Mineral Resources; 100000 Hanoi, Vietnam; e-mail: qdtin@monre.gov.vn

Received: 12 August 2021; accepted: 23 October 2021; first published online: 1 December 2021

Abstract: In northeastern Vietnam, the Khau Loc zone is considered to have high potential for lead-zinc mineralization. The lead isotope data for 18 galena samples and 18 ones of $\delta^{34}S$ isotope data (including galena and pyrite samples) were collected from lead-zinc ore deposits in some areas in the Khau Loc zone, including Phia Dam, Khuoi Man, Ban Lin, Lung Dam, and Ta Pan. These were employed to investigate the sulfur and lead isotope geochemical characteristics of Pb-Zn deposits and their significance in this study. The samples were analyzed using the LA-ICP-MS to show that the Pb isotopic ratios of $^{206}Pb/^{204}Pb$, $^{207}Pb/^{204}Pb$, and $^{208}Pb/^{204}Pb$ in the galena samples range from 17.8908 to 18.6012, 15.5794 to 16.1025, 38.4420 to 39.2118, with the average values of 18.296, 15.749, and 38.812, respectively. The pyrite and galena samples had the $\delta^{34}S$ isotope, ranging from 9.0 to 15.106. The sulfur isotope systematics implies that most of the lead-zinc ore formations originated from marine sedimentary evaporation deposits and magmatic intrusion-volcanic eruption sources rich in silica. The distribution of lead isotopic ratios had a well-defined cluster for each deposit, indicating the formation of lead-zinc deposits and lower crust and orogen trends. In addition, these findings of lead isotopic ratios and $\delta^{34}S$ isotopes proved that the Khau Loc zone is an activated structure with continuous growth in continental crust thickness during the early Proterozoic and Cenozoic periods. Furthermore, the study results also presented the evolution of material sources involved in the formation of lead-zinc ores in the Khau Loc zone.

Keywords: lead-zinc, sulfur and lead isotopes, Khau Loc zone, northeastern Vietnam

INTRODUCTION

In northeastern Vietnam, the Khau Loc zone is one with high potential for lead-zinc mineralization and has attracted considerable attention from geologists (Tri et al. 2011, Hung et al. 2020). In addition, lead-zinc mineralization plays a critical role in supplying the industry with useful metals because zinc, lead, and copper can be strongly contained together in polymetallic mineralization

https://doi.org/10.7494/geol.2021.47.3.143 ISSN 2299-8004 | e-ISSN 2353-0790 | Wydawnictwa AGH

in the deposits to be found in Phia Dam, Khuoi Man, Ban Lim, and Lung Dam (Quoc 2000, Tinh 2000, Graedel et al. 2015). These areas have been surveyed in geological mapping and mineral prospecting at 1:500,000–1:50,000 scale since 1965 (Dovzhikov 1965, Binh 2005, 2010, Bac 2011). The majority of them are located in lower and middle Devonian carbonate deposits with various parts of terrigenous and volcanic elements. They have been categorized by many Vietnamese researchers as being of the stratiform type (Duong 1990, Binh 2005, 2010, Bac 2011). In terms of the sediment-hosted massive sulfide deposit forms, Binh et al. (2005, 2010) suggested that it would be prudent to clarify the genesis of ore deposits. As for mineral deposits of multiple genetic types, their ore-forming products have major variations; however, most of these studies have been carried out based on the geological characteristics, their geochemistry as well as mineralization age. However, to date, not much attention has been paid to ore-forming material sources. In this paper, the lead and sulfur stable isotopes are used to reveal the source of sulfur and lead in the lead-zinc ore and to discuss the deposit's genesis.

The lead and sulfur isotopes of lead-zinc mineralization have been studied to understand the genesis of ore deposits and ore-forming material sources; therefore, geochemical isotope diagrams can be used successfully by geochemists to interpret ore-forming material sources and their genesis (Colemal 1977, Claypool et al. 1980, Chambers 1982, Sakai et al. 1982, 1984, Kerridge et al. 1983, Ueda & Sakai 1984, Chaussidon et al. 1989). Various discrimination plots are presented to discriminate the different material sources sequentially. The results of $\delta^{34}S$ isotope values on the genesis of ore deposits were shown in diagrams of Kerridge et al. (1988) and Ohmoto & Rye (1979). In contrast, ore-forming material sources were illustrated in the diagrams of Sakai et al. (1982, 1984) and Ueda & Sakai (1984). The analysis results of lead isotopes, including $^{206}Pb/^{204}Pb$, $^{207}Pb/^{204}Pb$, and $^{208}Pb/^{204}Pb$ expressed characteristics of material sources involved in ore formation that was presented by means of the schematic diagrams of Zartman & Doe (1981), Davies (1984), Newsom et al. (1986), Allegre et al. (1988), and Rudnick & Goldstein (1990). The ore-forming environmental settings and material sources were displayed in the diagrams of Zartman & Haines (1988).

GEOLOGICAL BACKGROUND

Geological setting

The geological structure of the Khau Loc zone is one part of the Viet Bac block that mainly developed from the formation of plateaus during the early-middle Paleozoic (Quoc et al. 2000, Tinh et al. 2000, Xuyen et al. 2000; Fig. 1).

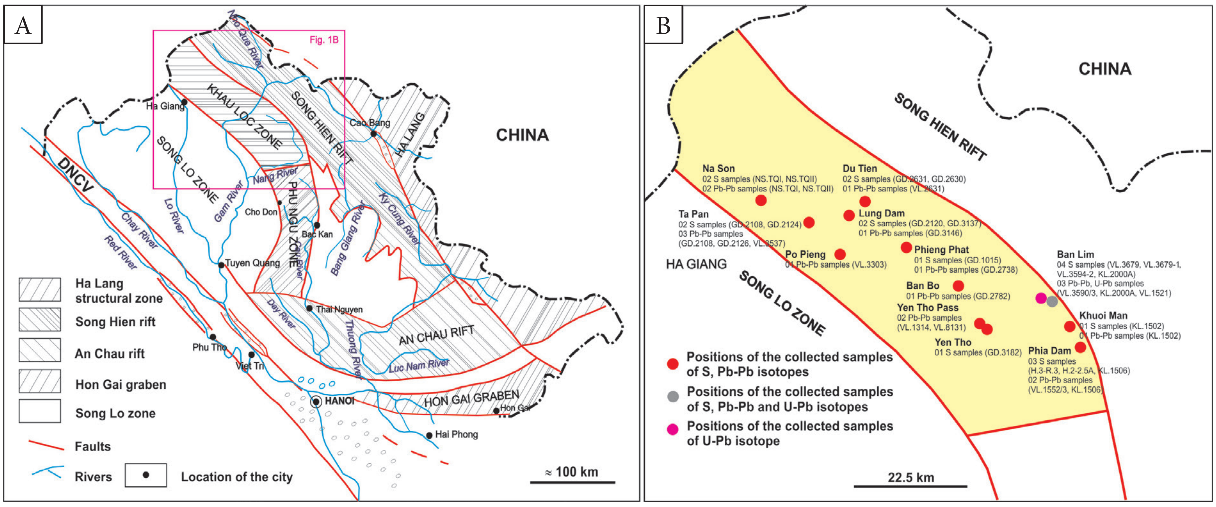

***Fig. 1.** Tectonic sketch map of northeastern Vietnam, showing the location of the Khau Loc zone (adapted from Tri et al. 2011) (A); locations of the lead-zinc deposits and occurrences in the Khau Loc zone (B)*

Furthermore, there was also a small volume of Carboniferous-Permian terrigenous, terrigenous-carbonate sediments distributed in the north-western part of the Khau Loc zone. In northeast Vietnam, the Khau Loc zone is separated by the Quan Ba-Ba Be deep fault in the West and divided from the Song Hien zone by the Song Nang-Ba Be deep fault in the East. This structure is separated from the Pho Ngu zone by the Ba Be strike-slip fault in the South. Moreover, the deep fault system in the center of the Khau Loc zone is characterized by open-circuit fault evidence, forming the late Permian-early Triassic granitoid massifs (Tinh et al. 2000, Xuyen et al. 2000, Binh 2005, 2010). Strike-slip fault systems such as the Song Gam and Du Gia-Minh Son faults divide the Khau Loc zone into three different blocks, showing different mineralizations in each block (Quoc et al. 2000, Tinh et al. 2000, Xuyen et al. 2000; Fig. 2).

The lithology of the study area is mainly dominated by quartz-sericite-chlorite schist, terrigenous bearing quartz sediments that were determined as early Proterozoic. Cambrian and Ordovician formations composed mainly of carbonate and marlstone. These formations are covered by Silurian rhyolite formation. The Devonian formation is distributed in small areas, and exposed along narrow basins filled with limestones and dolostones. The lead-zinc deposits are mainly restricted in Neoproterozoic and lower and middle Devonian formation (Quoc et al. 2000, Tinh et al. 2000, Xuyen et al. 2000; Fig. 2).

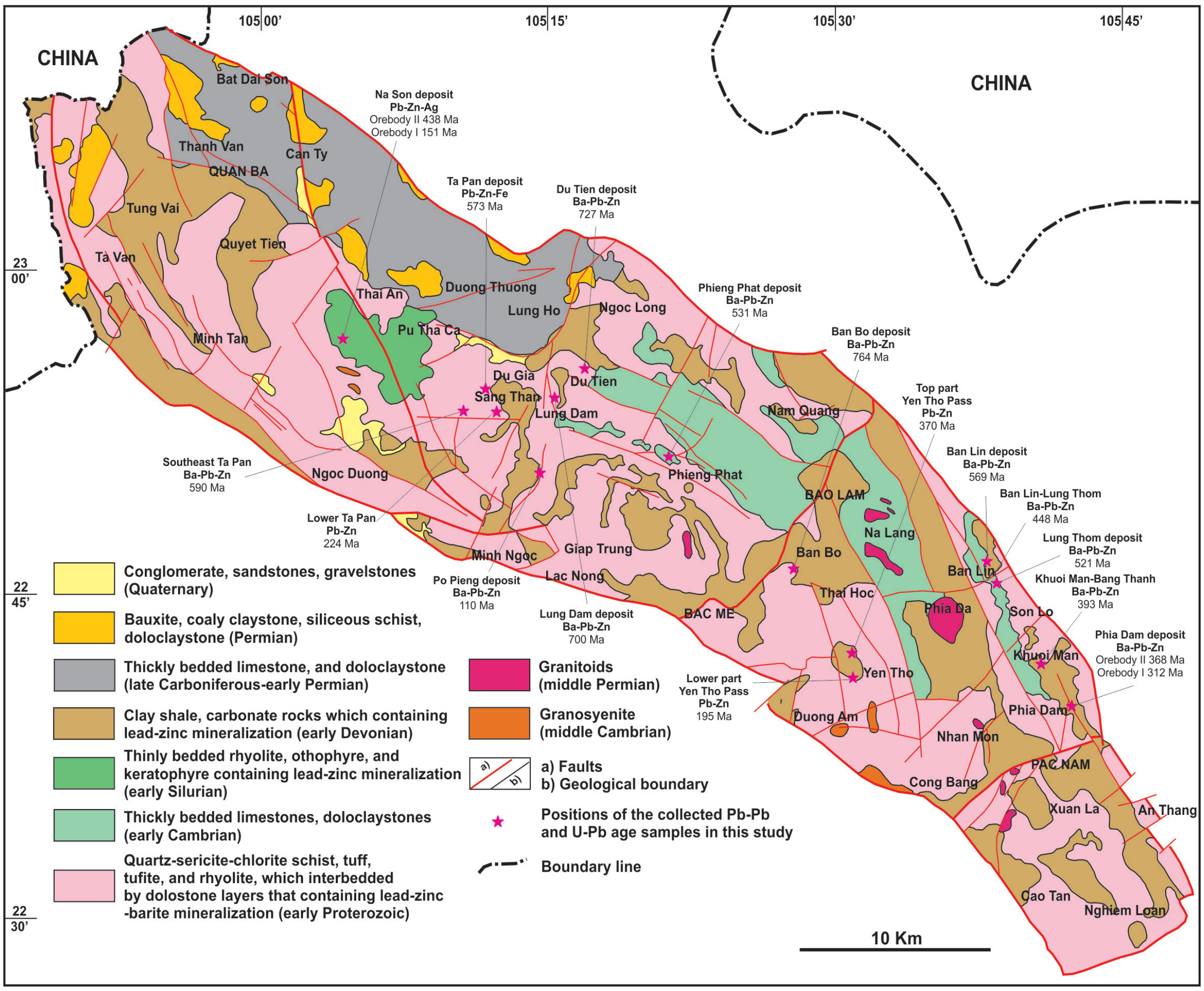

Fig. 2. *Simple geological map of the Khau Loc zone, northeastern Vietnam, showing the collected positions of lead-zinc samples (modified from Quoc et al. 2000, Tinh et al. 2000, Xuyen et al. 2000)*

Deposit geology

Most of the Pb-Zn deposits were found in the middle of the Khau Loc zone that is mainly restricted in the strata-bound brecciated dolostone (i.e., Du Tien, Lung Dam, Ta Pan, Ban Lin, Phieng Phat, and Yen Tho deposits), with minor terrigenous bearing quartz sediments (i.e., Ban Bo, Khuoi Man, and Phia Dam deposits) and rhyolite formation (i.e., Na Son deposit) (Duong 1990, Binh et al. 2005, 2010, Bac 2011; Fig. 2). In the Khau Loc zone, the Pb-Zn deposits mainly contain sphalerite, galena, barite, pyrite, and chalcopyrite, with minor pyrrhotite and andorite. The minerals of the gangue include primarily calcite and dolomite, supplemented by quartz, calcite, and minor fluorite. The modification of the host rock involves silicate dolomitization, pyritization, and baratization. Several stratiform, platy, nest-like, and lenticular types were found in the primary ore bodies. The ore textures are medium to coarse-grained, euhedral, and mainly brecciated ore structures, with massive minor vein and stockwork structures. The modification of the wall rock involves silicate dolomitization, pyritization, and baratization.

Mineralogy of lead-zinc ores

According to Binh et al. (2010), the mineralogy of lead-zinc ores in the study area is galena, sphalerite, barite, pyrite, chalcopyrite, minor pyrrhotite, andorite, and a few supergene minerals, including limonite and malachite. Sphalerite, smithsonite, hydrozincite, sheridanite, and zinc-bearing dolomite, and calcite are among the zinc-containing minerals discovered. Galena and minor quantities of anglesite and andorite are all lead-containing minerals. Limonite (which also includes lead and zinc), native silver, pyrite, minor quantities of chalcopyrite and enargite, quartz, chlorite, mica, feldspar, and essonite are among the other minerals found. Hydrothermal breccias also occur in this region. They appear as banded, broken veins or vein-like features.

As previously stated, lead-zinc ores are geographically associated with lower Devonian carbonate rocks and are sometimes restricted in Neoproterozoic formation; rock-forming minerals include calcite, dolomite, clay minerals group, quartz, barite, and organic material. In interaction with opaque minerals, rock-forming minerals often exhibit dissolution and embayment textures. The presence of sulfide minerals appears to be linked to the amount of quartz, barite, hydrothermal calcite, and dolomite in rocks and/or mineralization zones.

MATERIALS AND METHODOLOGY

We collected thirty lead-zinc ores samples from various deposits and ore occurrences; among them, 18 galena samples are used for testing lead-zinc isotopic analysis, and 18 galena and pyrite samples are used for testing sulfur isotopic analysis (Figs. 1B, 2). Of these, this study analyzed two galena samples from the Na Son deposit, three galena and pyrite samples from the Du Tien deposit, five galena and pyrite samples from the Ta Pan deposit, three galena samples of the Lung Dam deposit, one galena sample of the Po Pieng deposit, two galena and pyrite samples from the Phieng Phat deposit, one galena sample from the Ban Bo deposit, two galena samples from the Yen Tho Pass and one pyrite sample of the Yen Tho deposit, five galena and pyrite samples from the Ban Lin deposit, one galena sample from the Khuoi Man deposit, and four galena and pyrite samples from the Phia Dam deposits.

Sulfur isotope analysis

The sulfide minerals were isolated from typical ore samples obtained from the examined ore veins, and ore lens and sulfur isotope investigations were performed. Crushing, grinding, and sifting (from –250 to +125 m) were used to release unaltered pyrite and galena mineral particles, then hand-picked under a reflected light microscope. Finally, the mineral separates were powdered. The $\delta^{34}S$ ratios were analyzed at the University of Science and Technology of China using a EA1500 elemental analyzer connected to VG/Fisons/Micromass 'Isochrom-EA' system that was operated in the continuous He flow mode. The amount of the sample tested is determined by the sulfur concentration of the sulfide material. For sulfides having 50 wt.% S (pyrite, marcasite), an amount as little as 0.5 mg is employed; for sulfides containing 12–13 wt.% S, such as galena, the quantity tested is more than 2 mg. Before being thrown into a furnace at 1030°C, the samples are individually crimped in a tin capsule. The sample is flash combusted at 1800°C under helium atmosphere and with the simultaneous injection of O_2 into the system. The gases are subsequently oxidized, and the extra oxygen is absorbed in copper wires. The resultant gases are then separated in a chromatographic column, their peaks quantified, and the SO_2 gas is isolated to be analyzed directly in the mass spectrometer, all carried by He.

For the sulfide minerals, an accuracy of 0.1 for $\delta^{34}S$ has been achieved. The findings are related to Canyon Diablo Triolite. One standard is utilized to monitor the run at the start of the day and frequently during the run. Its work also includes checking to see if the surplus O_2 has been completely absorbed. In addition, six standards were utilized to calibrate the corrections to the raw values acquired for the samples. They span more than 50 degrees, from −32 to +20‰. For every five samples, one standard is analyzed to confirm or eventually adjust the calibration, and for every ten analyses, one blank is performed to "flush" the system.

Lead isotope analysis

The isotopic samples of Pb-Pb and U-Pb were analyzed with the LA-ICP-MS method at MC-A-ICP-MS Laboratory in the Institute of Geology and Geophysics, Chinese Academy of Sciences. To determine the isotope ratio of U-Pb, there was approximately 50 mg of rock and 50 mg of galena with the Pb-Pb isotope to be used. The samples were destroyed in a mixture of $HF\text{-}HClO_4$ in a Teflon beaker and placed in a sealed steel beaker at 180°C for six days to ensure complete digestion. Pb was separated and purified by the conventional cation-exchange technique with diluted HBr that was then measured on a Finnigan MAT-262 mass spectrometer at the University of Science and Technology of China. The standard sample NBS SRM-981 was analyzed with the results of $^{206}Pb/^{204}Pb$ = 18.640–18.08, $^{207}Pb/^{204}Pb$ = 15.741–15.758, and $^{208}Pb/^{204}Pb$ = 39.160–39.336.

RESULTS AND DISCUSSION

Ore mineralogy of the study samples

Calcite, dolomite, clay minerals, quartz, barite, and organic material are the rock-forming minerals in carbonate (Fig. 3A, B). The abundances of quartz, barite, hydrothermal calcite, and dolomite in rocks and/or mineralization zone seem to be related to the occurrence of sulfide minerals. Galena, sphalerite, barite, pyrite, chalcopyrite, minor pyrrhotite, andorite, and a few supergene minerals, including limonite and malachite, were included found in the analyzed samples (Fig. 3C–I).

Sphalerite and galena are typically found as anhedral crystals with grain diameters ranging from 0.3 to 2.5 mm in samples. They replace the previous rock-forming minerals and are intimately related to pyrite (Fig. 3D–I). It is typical to record the texture of sphalerite and galena filling in microcrack systems, which form veinlets or branches. Pyrite is most investigated samples are euhedral to subhedral, with grain sizes ranging from 0.1 to 2.5 mm. The pyrite rim is frequently eroded and replaced by sphalerite, suggesting that pyrite is the ore's oldest crystalline phase.

Sulfur and lead isotope compositions and their constraints on the ore genesis of the Pb-Zn deposits

18 galena samples were studied, and the results are provided in Table 1. The $\delta^{34}S$ values range from +9.00 to +15.106‰ (mean = 11.557 ±0.006, 1δ). The $\delta^{34}S$ values can be used to discuss the genesis of the lead-zinc deposits into the three following groups, including hydrothermal-sedimentary, hydrothermal-volcanic, and hydrothermal types (Tab. 1).

The results of the isotopic ratio measurements are illustrated in Table 2. Overall, lead isotope ratios are clustered between 17.8908 and 18.6012 (average 18.2960 ±0.0012), 15.5794 to 16.1025 (average 15.7489 ±0.0010), and 38.442 to 39.2118 (average 38.8118 ±0.0031) for $^{206}Pb/^{204}Pb$, $^{207}Pb/^{204}Pb$ and $^{208}Pb/^{204}Pb$, respectively (Tab. 2). Three outliers in the Khau Loc data deviated from the overall $^{206}Pb/^{204}Pb$ trend and are discussed below.

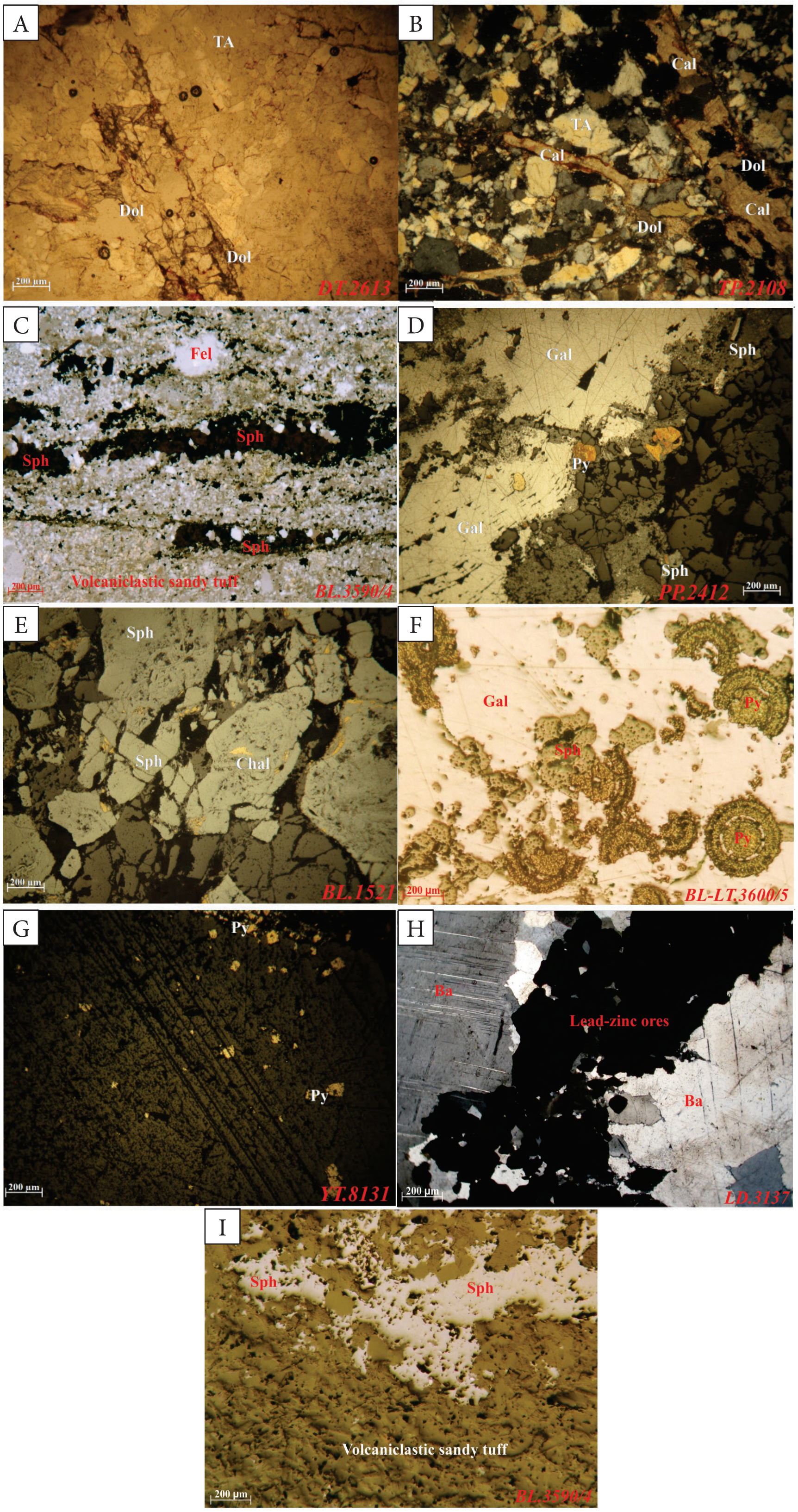

Fig. 3. *Representative photos of the host rocks and Pb-Zn ores: quartz-calcite-dolomite schist (A, B); sphalerite ore veins bearing volcanic sandy tuff (C, I); remnant colloform pyrite at the Ban Lin-Lung Thom deposit (F); mineral assemblages of the studied Pb-Zn ores (D, E, G, H). DT, TP, BL, PP, BL-LT, YT, LD – Du Tien, Ta Pan, Ban Lin, Phieng Phat, Ban Lin-Lung Thom, Yen Tho, Lung Dam deposits, respectively. Py – pyrite, Chal – chalcopyrite, Sph – sphalerite, Gal – galena, Ba – barite, Dol – dolomite, Cal – calcite, TA – quartz, Fel – feldspar*

Table 1
The $\delta^{34}S$ [‰] isotopes in lead-zinc deposits and occurrences

Sample location	Sample numbers	$\delta^{34}S$ [‰]	Error (1δ)	Ore type
Du Tien	GD.2631	11.876	0.009	hydrothermal-sedimentary
	GD.2630	12.303	0.005	
Lung Dam	GD.2120	10.809	0.002	hydrothermal-sedimentary
	GD.3137	11.808	0.006	
Ta Pan	GD.2108	15.106	0.006	hydrothermal-sedimentary
Southeast Ta Pan	GD.2124	11.665	0.008	hydrothermal-sedimentary
Phieng Phat	GD.1015	10.706	0.005	hydrothermal-sedimentary
Yen Tho	GD.3182	12.015	0.008	hydrothermals
Na Son	NS.TQI	9.687	0.004	hydrothermal-volcanics
	NS.TQII	11.034	0.006	hydrothermals
Ban Lin	VL.3679	11.1	Orebody 1	hydrothermal-volcanics
	VL.3679-1	13.3		
	VL.3594-2	10.1	Orebody 2	
Phia Dam	H.3-R.3	9.5	Orebody II	hydrothermal-sedimentary
	H.2-2.5A	9.0		
Southern Ban Lin-Lung Thom	KL.2000A	13.632	0.005	hydrothermal-sedimentary
Khuoi Man-Bang Thanh	KL.1502	12.703	0.006	hydrothermal-sedimentary
Lower part of the Phia Dam	KL.1506	11.678	0.006	hydrothermal-sedimentary

Lead-zinc-barite and lead-zinc ores of hydrothermal-sedimentary type were identified as the most popular mineralization in the Khau Loc zone with their main concentration in the central and southern parts of the structure, characterized by the lead-zinc seams which are distributed in quartz-sericite schists and limestone-dolostone of the Neoproterozoic and Devonian strata, and a small volume of early Carboniferous formation overlapping these formations (Fig. 2). The ore-forming age was established based on the mineralization model ages of Pb/Pb and U/Pb in the eruptive formations containing these ores, and ore-forming origin is determined depending on $\delta^{34}S$ isotope values as shown in Tables 1 and 2.

The schematic of the isotope values of $\delta^{34}S$ indicating ore-forming material sources is shown in Figure 4. From this diagram of ore-forming origins, it can be concluded that most of the lead-zinc ore formations started from marine sedimentary evaporation deposits and magmatic intrusion-volcanic eruption sources rich in silica.

The main types of ore-forming origin are plotted in Figure 5. It is indicated that lead-zinc ore formations were generally originated from shallow sources, basically related to sediment-hosted massive sulfide deposits such as Red-bed, and Mississippi-valley types. These results are similar to the previous research of Hoa et al. (2008), Ishihara et al. (2010), and Bac (2011).

Formations of hydrothermal-volcanic origin in the Khau Loc zone are not very concentrated; instead, they are popular in the Na Son formation and a small part of eruptive rhyolite formations in the Ban Lin area (Figs. 2–6). The main characteristic of these formations is the presence of lead-zinc-silver ore. An analysis of the results of sulfur and lead isotopic ratios of lead-zinc ores collected from the Na Son formation and U/Pb from the Ban Lin rhyolite formation revealed that lead-zinc ores from the two places have similar ages (Tab. 2). The analysis results of $\delta^{34}S$ isotopes from the Na Son deposit, as shown in Figure 4, proved that they have such material origins as volcanic sources and intrusive ones. Their distribution characteristics meant that there is a relationship between them and the eruptive source of the Na Son formation.

Table 2
Analyzed results of lead isotope ratios in lead-zinc deposits and occurrences

Ore deposits	Sample	$^{206}Pb/^{204}Pb$	Error (2δ)	$^{207}Pb/^{204}Pb$	Error (2δ)	$^{208}Pb/^{204}Pb$	Error (2δ)	Lead model age	μ value
Ban Bo	GD.2782	18.3293	0.0034	15.8930	0.00047	39.0144	0.0149	764	11.05
Du Tien	VL.2631	18.3082	0.0011	15.8624	0.0011	38.9018	0.0031	727	10.91
Lung Dam	GD.3146	18.3414	0.0014	15.8596	0.0014	38.9708	0.0035	700	10.88
Southeast Ta Pan	GD.2126	18.1617	0.0012	15.7257	0.0011	38.4684	0.0030	590	10.32
Ta Pan deposit	GD.2108	18.1608	0.0016	15.7177	0.0015	38.4420	0.0038	573	10.28
Orebody III Ban Lin	VL.3590/3	18.3106	0.0014	15.7720	0.0014	38.9714	0.0013	569	10.48
Lung Thom	KL.2000A	17.8908	0.0012	15.6785	0.0013	38.5320	0.0042	521	9.36
Ban Lin-Lung Thom	VL.1521	18.3928	0.0009	15.7373	0.0008	38.7995	0.0021	448	10.29
Phieng Phat	GD.2738	18.2087	0.0007	15.7119	0.0006	38.4546	0.0015	531	10.24
Orebody II Na Son	NS.TQII	18.5641	0.0013	15.7968	0.0012	39.2118	0.0020	438	10.51
Khuoi Man-Bang Thanh	KL.1502	17.9626	0.0013	16.1025	0.0012	38.5283	0.0031	393	9.25
Top part of the Yen Tho Pass	VL.1314	18.4365	0.0013	15.7129	0.0011	38.8642	0.0024	370	10.17
Orebody II Phia Dam	VL.1552/3	18.6012	0.0011	15.7733	0.0009	39.1024	0.0026	368	10.40
Orebody I Phia Dam	KL.1506	18.1073	0.0012	15.7526	0.0007	38.8136	0.0032	312	10.12
Lower part of the Ta Pan	VL.3537	18.3362	0.0008	15.6030	0.0008	38.7951	0.0016	224	9.71
Lower part of the Yen Tho Pass	VL.8131	18.3085	0.0008	15.5794	0.0010	38.8992	0.0018	195	9.61
Orebody I Na Son	NS.TQI	18.4615	0.0011	15.6138	0.0011	39.0015	0.0014	151	9.73
Po Pieng	VL.3303	18.4459	0.0008	15.5887	0.0007	38.8426	0.0014	110	9.26

Note: The error (2δ) is the standard deviation of data analysis samples; it is obtained by calculating data analysis samples following the normal standard distribution model (it means that the data sample is changing around 95% of confidence interval). The μ value is the ratio of ^{238}U and ^{204}Pb ($\mu = ^{238}U/^{204}Pb$).

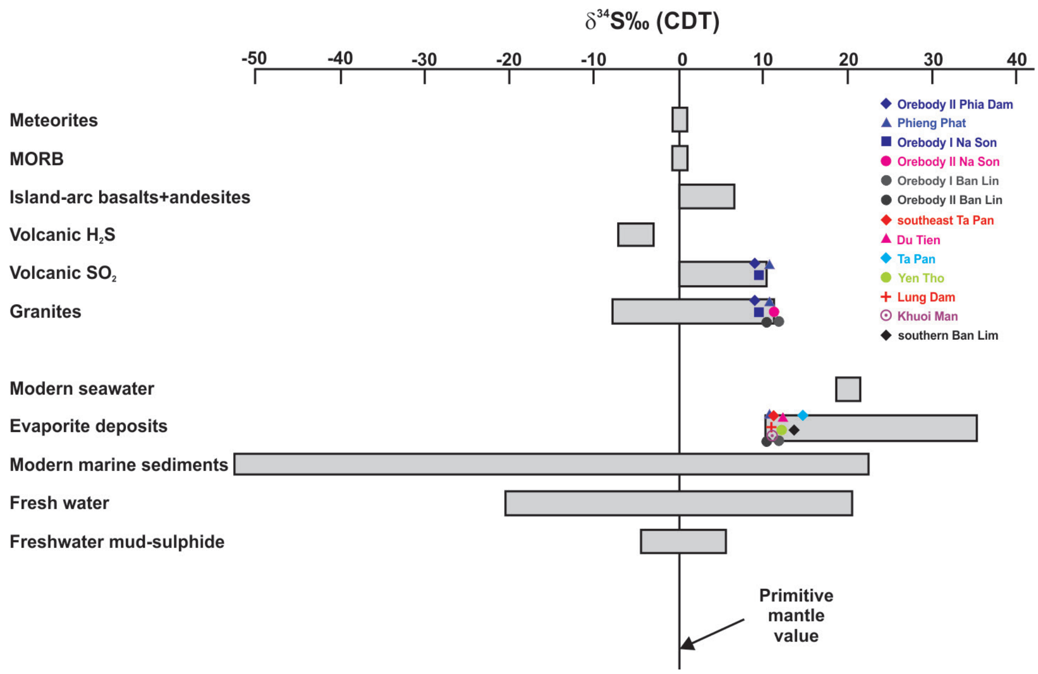

Fig. 4. *Natural sulfur isotope reservoirs, showing lead-zinc forming material sources in the Khau Loc zone (data from Coleman 1977, Claypool et al. 1980, Chambers 1982, Sakai et al. 1982, Kerridge et al. 1983, Ueda & Sakai 1984, Chausidon et al. 1989)*

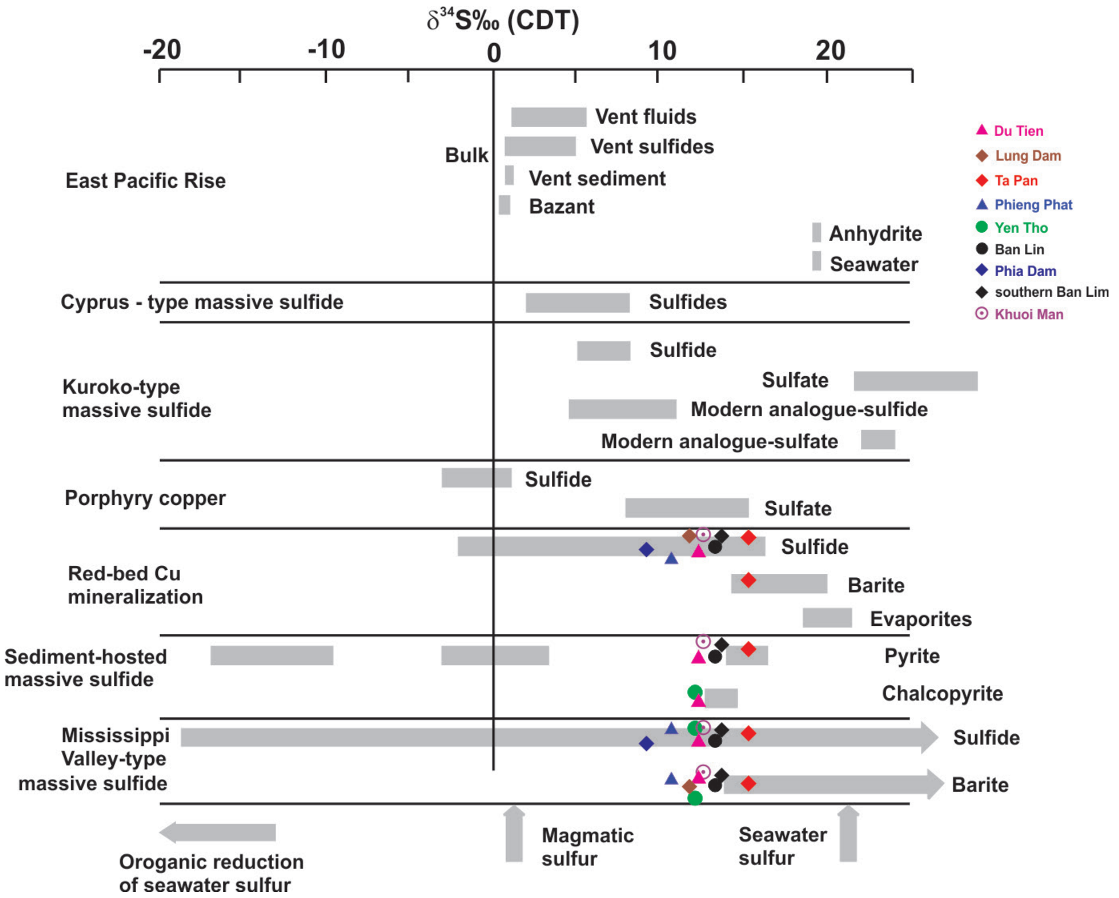

Fig. 5. *The $\delta^{34}S$ values for sulfur-bearing minerals in hydrothermal deposits, showing the lead-zinc deposits of the Khau Loc zone (data from Ohmoto & Rye 1979, Eldridge et al. 1988, Kerridge et al. 1988, and Naylor et al. 1989)*

In place of frequent denotation, lead-zinc mineralization of a hydrothermal origin is mainly distributed over existing paths during previous mineralization ages, adjacent to ore fields and deposits. Their scale is small, as seen in orebody II Na Son, Po Pieng, and Yen Tho (Fig. 6). The analysis results of $\delta^{34}S$ isotope values showed that these ore formations are still shallow hydrothermal sources and related to intrusive and volcanic formations. They were formed in the late Mesozoic era (Jurassic to Cretaceous) (Tab. 2).

Based on the lead isotope ratios in ore deposits and occurrences in the Khau Loc zone, as shown in Table 2, schematic diagrams of lead-zinc ore formation and development characteristics throughout different mineralization ages were synthesized and plotted.

The results of isotope ratios of $^{206}Pb/^{204}Pb$, $^{207}Pb/^{204}Pb$, and $^{208}Pb/^{204}Pb$ of the ore deposits and occurrences in the Khau Loc zone are plotted in the diagrams of Zartman & Haines (1988) (Fig. 7) on the mineral deposit setting and location of the material supply sources through the metallogenic ages from Proterozoic-Cambrian to Paleozoic, and Mesozoic eras are mentioned as followed.

The Proterozoic-Cambrian metallogeny, developing with many lead-zinc deposits and lead-zinc occurrences as lead-zinc ore fields in the Du Tien, Lung Dam, Ta Pan, Ban Bo, Ban Lin-Lung Thom, and Phieng Phat deposits, are presented in Figure 7A, B. The Paleozoic metallogeny with lead-zinc deposits of the Na Son, Ban Lin types during the eruption stage, namely Yen Tho Pass, Khuoi Man, Phia Dam, are illustrated in Figure 7C, D. Besides, the late Mesozoic metallogeny with low-part ore deposits of Na Son, Ta Pan, Po Pieng, and Yen Tho are plotted in Figure 7E, F.

The plumbotectonics model can be used to constrain the source of Pb (Zartman & Doe 1981). As shown in the $^{208}Pb/^{204}Pb$ vs. $^{206}Pb/^{204}Pb$ and

$^{207}Pb/^{204}Pb$ vs. $^{206}Pb/^{204}Pb$ diagrams (Fig. 7), the Pb isotopic composition data for all sulfides obtained in this study were all projected on the lower crust, excepted the Pb isotopic composition data of southeast Ta Pan, Ta Pan, Phieng Phat, and lower part of the Ta Pan, Yen Tho Pass, orebody I Na Son, Po Pieng deposits to be projected on the orogenic setting. This implies that there would be a possibility of the imperfect mixing of normal lead in different source regions. Therefore, it is pointed out from the above Pb isotopic composition characteristics that the lead sources are not only the lower crust but also some other source regions, for example, the basement of the Caledonian and Yanshanian orogenic zones (Velasco et al. 1996, Golonka et al. 2006, Hoa et al. 2008, Hung 2010, Milot et al. 2021).

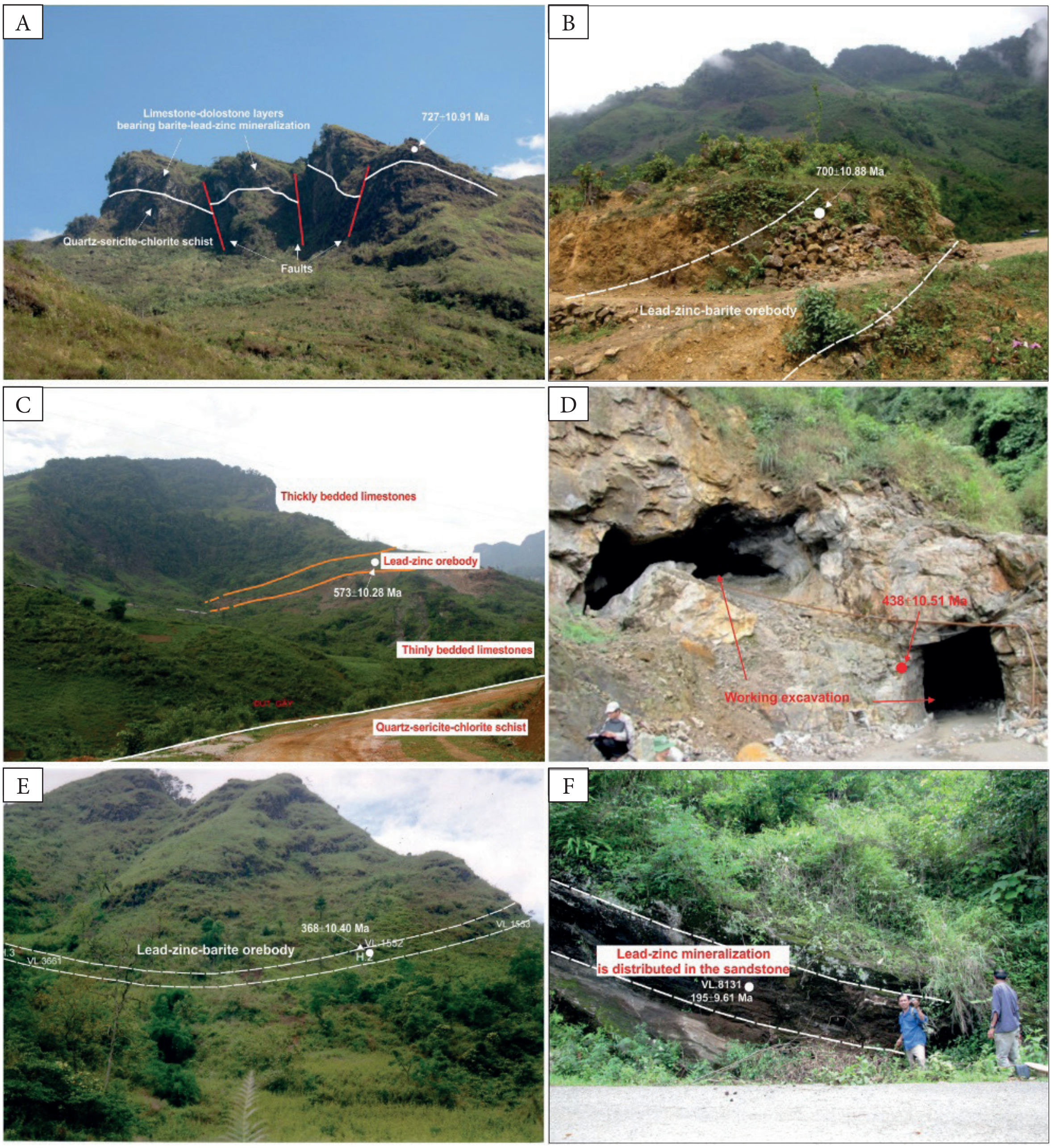

Fig. 6. *Lead-zinc mineralization and their positions (small colored circles) of the collected dating samples in the Khau Loc zone, northeast Vietnam: A) barite-lead-zinc mineralization in the Du Tien occurrence (727 ±10.91 Ma); B) lead-zinc-barite orebody, Lung Dam deposit (700 ±10.88 Ma); C) lead-zinc orebody, Ta Pan deposit (573 ±10.28 Ma); D) lead-zinc-sliver orebody II, Na Son deposit (438 ±10.51 Ma); E) lead-zinc-sliver orebody II, Phia Dam deposit (368 ±10.40 Ma); F) lead-zinc mineralization at the lower part of the Yen Tho Pass (195 ±9.61 Ma)*

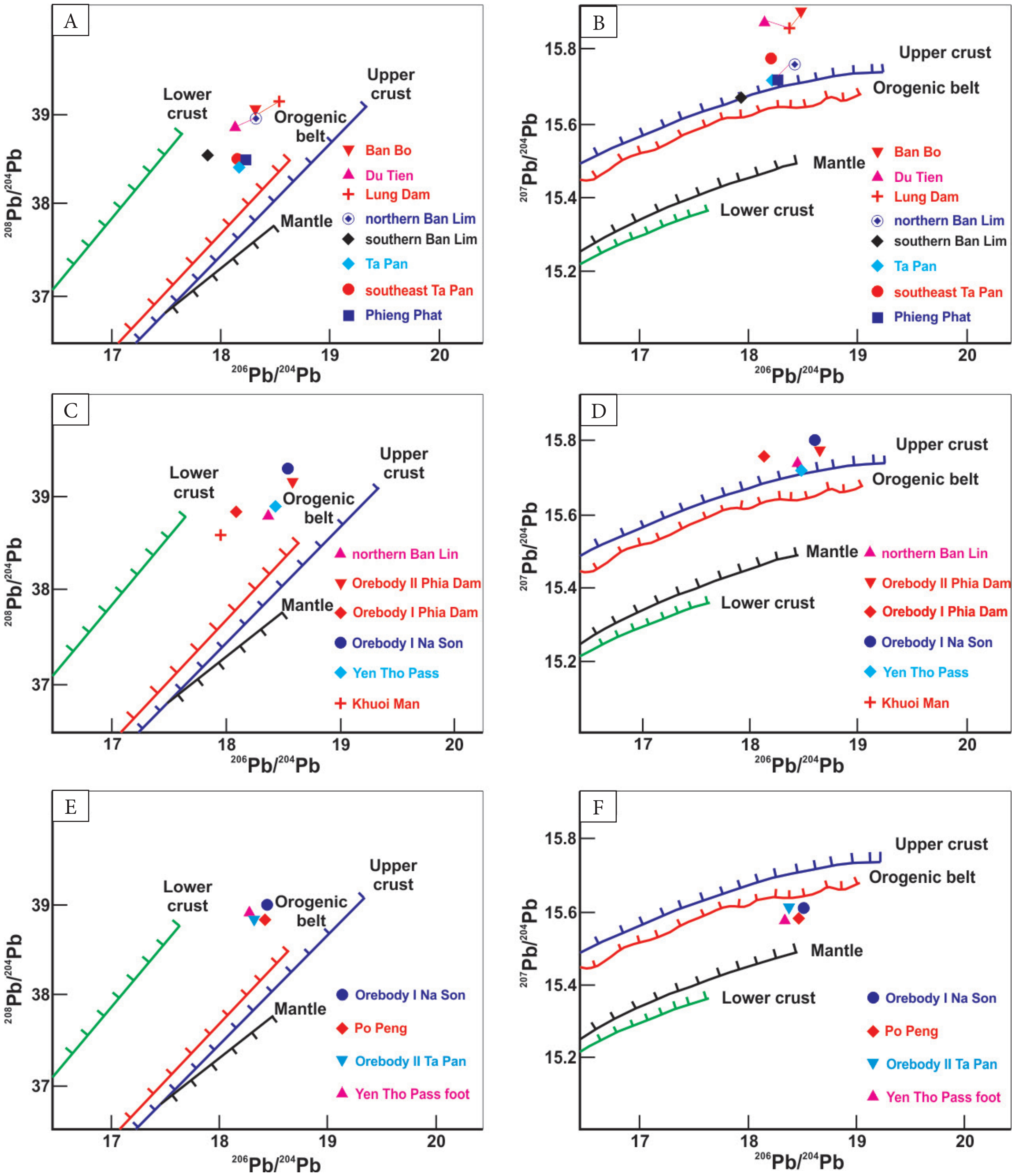

Fig. 7. *Lead isotope evolution curves for the upper crust, lower crust, mantle, and orogen plotted for $^{208}Pb/^{204}Pb$ vs. $^{206}Pb/^{204}Pb$ (A) and $^{207}Pb/^{204}Pb$ vs. $^{206}Pb/^{204}Pb$ (B) for plumbotectonics version IV (Zartman and Haines 1988). The ticks on each curve are at 100 Ma intervals of the ore deposits and occurrences in the Khau Loc zone during the Proterozoic-Cambrian (A, B), Paleozoic (C, D), and late Mesozoic (E, F) metallogeny*

From these diagrams, it can be seen that there has been an evolution of the material supply sources gradually shifting to the deep sources of the lower crust and forming in the orogenic settings. Furthermore, Allegre's et al. (1988) schematic also presented the characteristics of material sources forming lead-zinc ores in the Khau Loc zone as shown in Figure 8 with the mineralization ages starting from Proterozoic-Cambrian to Paleozoic and late Mesozoic eras with the above-discussed ore deposits and occurrences.

Based on the sulfur and lead isotope analysis of the Pb-Zn deposits and their occurrences in the Khau Loc zone, the source of ore-forming materials mainly originated from the lower crust and orogenic field. According to Table 2, it is inferred that ore-forming material, which was derived predominantly from basement rock and partially from Devonian carbonaceous rocks, is the source of the abundance of Pb-Zn mineralization of strata in the northeast margin of the Khau Loc region. Otherwise, rich in organic matter may be produced by carbonaceous rocks. The decomposition of organic matter is helpful for sulfate reduction (Velasco et al. 1996, Xue et al. 2007, Sangster et al. 2011, Duan et al. 2016, Gill et al. 2019, Ünal-Çakır 2020).

The ore-forming processes of Pb-Zn deposits and events can be summarized by means of an overview. Pb and Zn were collected by underground geothermal brine in the basement rock and carbonaceous rocks, with the Devonian dolomite dissolved. As ore-forming fluid migrates to the organic matter-rich dolomite breccia belt, ore forming matters precipitate Pb and Zn due to reduction, with the formation of hydrothermal dolomite.

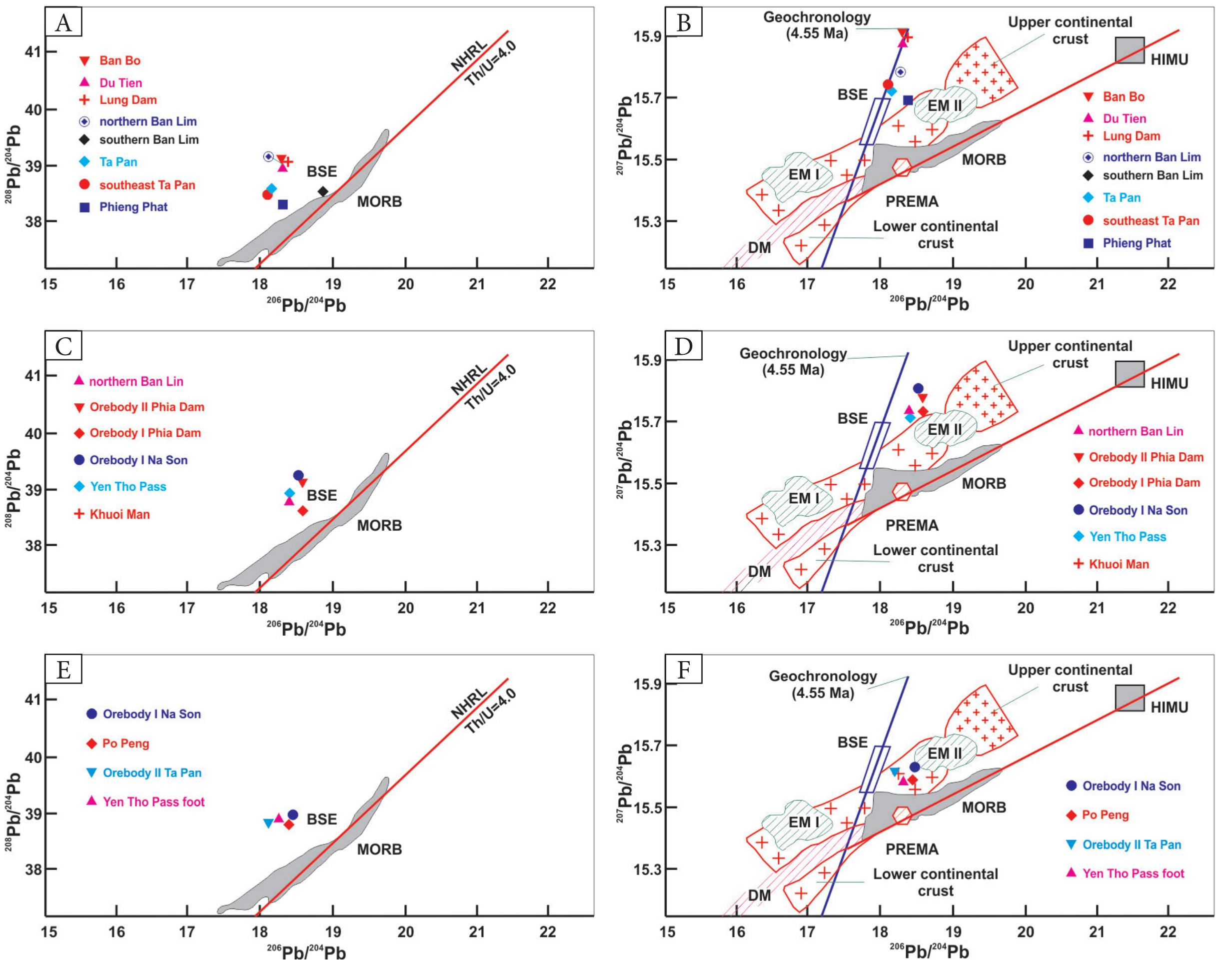

Fig. 8. The $^{208}Pb/^{204}Pb$ vs. $^{206}Pb/^{204}Pb$ isotope correlation diagram showing the position of the northern hemisphere reference line (NHRL) with Th/U = 4.0. The bulk silicate Earth value (BSE) is from Allegre et al. (1988). The field of MORB is described with a gray-hatched pattern. The $^{207}Pb/^{204}Pb$ vs. $^{206}Pb/^{204}Pb$ isotope correlation diagram illustrating the position of the northern hemisphere reference line (NHRL), the slope of which has an age significance of 1.77 Ga, and the geochronology and corresponding positions of Pb-Zn ore deposits in the Khau Loc zone during the Proterozoic-Cambrian (A, B), Paleozoic (C, D), and late Mesozoic (E, F) metallogeny (HIMU-Mantle with high U/Pb ratio; EM I and EM II-Enriched mantle)

CONCLUSIONS

The sulfur and lead isotopes of Pb-Zn deposits in the Khau Loc zone, northeastern Vietnam have been used to investigate the genesis of lead-zinc deposits and ore-forming material sources. The following conclusions can be drawn.

Based on lead isotope analysis, the results show that the ore formations of the Neoproterozoic and Cambrian periods have material sources involved in ore-forming all fall into the large silicate field of the earth's crust, with the Ban Lin-Lung Thom and Phieng Phat ore fields displaying rich mantle sources. However, the material sources involved in the Cambrian formations are closer to rich mantle sources than those in the Neoproterozoic, such as the Du Tien, Lung Dam, Ta Pan, and Ban Bo deposits. The ore formations in the Ordovician, Silurian, and Devonian mineralization stages have a deeper distribution of ore-forming materials than the Neoproterozoic and Cambrian formations, in which lead-zinc mineralization of this stage display a rich mantle source. The ore formations in the Jurassic-Cretaceous mineralization stage in the lower part of the Na Son, Po Pieng-Minh Son, Yen Tho, and Ta Pan deposits are all formed from the lower crust in the context of tectonic activation.

The $\delta^{34}S$ values of the Pb-Zn ore formations in the Devonian are extremely positive, reflecting the ore-forming environment in shallow conditions. Most of the sulfur isotope values fall into the field of marine sedimentary evaporation deposits (sediment-hosted massive sulfide deposits) and partly relate to intrusive volcanic formations and volcanic silica sources.

The material source involved in forming lead-zinc-barite and lead-zinc ores of the Khau Loc structure in the Neoproterozoic and Cambrian are characterized by a source between the upper and lower crust. The barite-lead-zinc ore formations in the Ordovician, Silurian, and Devonian mainly reflect the material source of the lower crust. The ore-mineralized formations in the Jurassic and Cretaceous originated from the lower crust in the context of tectonic activation. These indicate that the evolution of ore-forming materials for mineralization is increasingly at a deeper source, an essential fact to understand the mineralization potential involved.

The authors would like to thank the Reviewers and the Editors for their thoughtful and constructive comments that greatly improved the manuscript.

REFERENCES

Allegre C.J., Lewin E. & Dupre B., 1988. A coherent crust-mantle model for the uranium-thorium-lead isotopic system. *Chemical Geology*, 70, 211–234. https://doi.org/10.1016/0009-2541(88)90094-0.

Bac D.T., 2011. *Research on characteristics and distribution regularities of lead-zinc metallogenic formations in the Viet Bac area, Northern Vietnam*. University of Mining and Geology, Hanoi [Ph.D. Thesis] [Bắc D.T., 2011. *Nghiên cứu đặc điểm và sự phân bố sinh khoáng chì-kẽm vùng Việt Bắc, miền Bắc Việt Nam*. Luận án tiến sỹ, Đại học Mỏ-Địa chất].

Binh D.Q., Cuong D.Q., Chinh K.T., Hung N.M. & Que N.T., 2005. *Report on prospective results of lead-zinc, gold, and accompanying minerals of the Phia Da-Na Cang area, Cao Bang-Bac Kan provinces*. Vietnam Institute of Geosciences and Mineral Resources, Hanoi [Bình D.Q., Cường D.Q., Chính K.T., Hùng N.M. & Quế N.T., 2005. *Báo cáo kết quả tìm kiếm quặng chì-kẽm, vàng và các khoáng sản đi kèm vùng Phi Dạ-Na Cang, Cao Bằng-Bắc Kạn*. Viện Khoa học Địa chất và Khoáng sản].

Binh D.Q., Cuong D.Q., Dong N.C., De P.Q., Linh N.T.H., Que N.T. & San V.T., 2010. *Report on prospective results of copper, lead-zinc, and accompanying minerals of the Quang Ba-Pac Nam area, Ha Giang province*. Vietnam Institute of Geosciences and Mineral Resources, Hanoi [Bình D.Q., Cường D.Q., Đồng N.C., Đệ P.Q., Linh N.T.H. & Quế N.T., 2010. *Báo cáo kết quả tìm kiếm quặng đồng, chì-kẽm và các khoáng sản đi kèm vùng Quảng Bạ-Pắc Nậm, Hà Giang*. Viện Khoa học Địa chất và Khoáng sản].

Chambers L.A., 1982. Sulfur isotope study of a modem intertidal environment and the interpretation of ancient sulfides. *Geochimica et Cosmochimica Acta*, 46, 721–728.

Chaussidon M., Albarede F. & Sheppard S.M.F., 1989. Sulphur isotope variations in the mantle from ion microprobe analyses of micro-sulphide inclusions. *Earth and Planetary Science Letters*, 92, 144–156. https://doi.org/10.1016/0012-821X(89)90042-3.

Claypool G.E., Helser W.T., Kaplan I.R., Sakai H. & Zak I., 1980. The age curves of sulfur and oxygen isotopes in marine sulfate and their mutual interpretation. *Chemical Geology*, 28, 199–260. https://doi.org/10.1016/0009-2541(80)90047-9.

Coleman M.L., 1977. Sulphur isotopes in petrology. *Journal of the Geological Society*, 133, 593–608. https://doi.org/10.1144/gsjgs.133.6.0593.

Davies G.F., 1984. Geophysical and Isotopic Constraints on Mantle Convection-an Interim Synthesis. *Journal of Geophysical Research*, 89 (NB7), 6017–6040. https://doi.org/10.1029/JB089iB07p06017.

Dovzhikov A.Ye. (ed.), 1965. *Geology of North Vietnam. Explanatory note of the Geological Map of North Vietnam at 1:500,000 scale* [Довжиков А.Е. (ред.), 1965. *Геология Северного Вьетнама. Объяснительная записка к геологической карте Северного Вьетнама. Масштаб 1:500 000*]. Geological Department of Vietnam, Hanoi.

Duan J., Tang J. & Lin B., 2016. Zinc and lead isotope signatures of the Zhaxikang Pb-Zn deposit, South Tibet: Implications for the source of the ore-forming metals. *Ore Geology Reviews*, 78, 58–68. https://doi.org/10.1016/j.oregeorev.2016.03.019.

Duong T.V., 1990. *Complex-Ore Fields in Northeastern Vietnam: Geologic Structure and Formation Conditions*. Baku State University, Baku [extended abstract candidate of sciences (geology and minerals) dissertation].

Eldridge C.S., Compston W., Williams I.S., Both R.A., Walshe J.L. & Ohmoto H., 1988. Sulfur isotope variability in sediment-hosted massive sulfide deposits as determined using the ion-microprobe, SHRIMP: I. An example from the Rammelsberg orebody. *Economic Geology*, 83, 443–449. https://doi.org/10.2113/gsecongeo.83.2.443.

Gill S., Piercey S., Layne G.D. & Piercey G.D., 2019. Sulphur and lead isotope geochemistry of sulphide minerals from the Zn-Pb-Cu-Ag-Au Lemarchant volcanogenic massive sulphide (VMS) deposit, Newfoundland, Canada. *Ore Geology Reviews*, 104, 422–435. https://doi.org/10.1016/j.oregeorev.2018.11.008.

Golonka J., Krobicki M., Pająk J, Giang N.V. & Zuchiewicz W., 2006. *Global plate tectonics and paleogeography of Southeast Asia*. Faculty of Geology, Geophysics and Environmental Protection, AGH University of Science and Technology, Kraków.

Graedel T.E., Harper E.M., Nassar N.T. & Reck B.K., 2015. On the Materials Basis of Modern Society. *Proceedings of the National Academy of Sciences*, 112, 4257–4262. https://doi.org/10.1073/pnas.1312752110.

Hoa T.T., Izokh A.E., Polyakov G.V., Borisenko A.S., Anh T.T., Balykin P.A., Phuong N.T., Rudnev S.N., Van V.V. & Nien B.A., 2008. Permo-Triassic magmatism and metallogeny of Northern Vietnam in relation to the Emeishan plume. *Russian Geology and Geophysics,* 49, 480–491. https://doi.org/10.1016/j.rgg.2008.06.005.

Hung K.T., 2010. Overview of magmatism in Northwestern Vietnam. *Annales Societatis Geologorum Poloniae*, 80, 125–186.

Hung K.T., Sang P.N., Phuong N., Linh V.T. & Sang B.V., 2020. Statistical evaluation of the geochemical data for prospecting polymetallic mineralization in the Suoi Thau-Sang Than region, Northeast Vietnam. *Geology, Geophysics and Environment*, 46, 285–299. https://doi.org/10.7494/geol.2020.46.4.285.

Ishihara S., Tuan-Anh T., Yasushi W. & Trong-Hoa T., 2010. Chemical characteristics of lead-zinc ores from North Vietnam, with a special attention to the in contents. *Bulletin of the Geological Survey of Japan*, 61, 307–23. https://doi.org/10.9795/bullgsj.61.307.

Kerridge J.F., Chang S. & Shipp R., 1988. Deuterium exchange during acid-demineralization. *Geochimica et Cosmochimica Acta*, 52, 2251–2255. https://doi.org/10.1016/0016-7037(88)90127-5.

Kerridge J.F., Haymon R.M. & Kastner M., 1983. Sulfur isotope systematics at the 21°N site, East Pacific Rise. *Earth and Planetary Science Letters*, 66, 91–100. https://doi.org/10.1016/0012-821X(83)90128-0.

Milot J., Blichert-Toft J., Sanz M.A., Fetter N., Télouk P. & Albarède F., 2021. The significance of galena Pb model ages and the formation of large Pb-Zn sedimentary deposits. *Chemical Geology*, 583, 120–444. https://doi.org/10.1016/j.chemgeo.2021.120444.

Naylor H., Turrier P., Vaughan D.J., Boyce A.J. & Fallick A.E., 1989. Genetic studies of redbed mineralization in the Triassic of the Cheshire basin, northwest England. *Journal of the Geological Society*, 146, 685–699. https://doi.org/10.1144/gsjgs.146.4.0685.

Newsom H.E., White W.M., Jochum K.P. & Hofmann A.W., 1986. Siderophile and Chalcophile Element Abundances in Oceanic Basalts, Pb-Isotope Evolution and Growth of the Earth's Core. *Earth and Planetary Science Letters,* 80, 299–313. https://doi.org/10.1016/0012-821X(86)90112-3.

Ohmoto H. & Rye R.O., 1979. Isotopes of sulfur and carbon. [in:] Barnes H.L. (ed.), *Geochemistry of Hydrothermal Ore Deposits*, Wiley, New York, 509–567.

Quoc N.K. (ed.), 2000. *Report on results of geological mapping and mineral investigation of Bac Kan sheet at 1:200.000 scale*. Geological Department of Vietnam, Hanoi [Quốc N.K. (chủ biên), 2000. *Báo cáo kết quả đo vẽ bản đồ và tìm kiếm khoáng sản tờ Bắc Kạn tỷ lệ 1:200.000*. Lưu trữ Cục địa chất và khoáng sản Việt Nam, Hà Nội].

Rudnick R.L. & Goldstein S.L., 1990. The Pb isotopic composition of lower crustal xenoliths and the evolution of lower crustal Pb. *Earth and Planetary Science Letters,* 98, 192–207. https://doi.org/10.1016/0012-821X(90)90059-7.

Sakai H., Casadevall T.J. & Moore J.G., 1982. Chemistry and isotope ratios of sulfur in basalts and volcanic gases at Kilauea volcano, Hawaii. *Geochimica et Cosmochimica Acta*, 46, 729–738. https://doi.org/10.1016/0016-7037(82)90024-2.

Sakai H., Des Maris D.J., Ueda A. & Moore J.G., 1984. Concentrations and isotope ratios of carbon, nitrogen, and sulfur in ocean-floor basalts and volcanic gases at Kilauea volcano, Hawaii. *Geochimica et Cosmochimica Acta*, 48, 2433–2441. https://doi.org/10.1016/0016-7037(84)90295-3.

Sangster D., Outridge P.M. & Davis W., 2011. Stable lead isotope characteristics of lead ore deposits of environmental significance. *Environmental Reviews*, 8, 115–147. https://doi.org/10.1139/a00-008.

Tinh H.X. (ed.), 2000. *Report on results of geological mapping and mineral investigation of Bao Lac sheet at 1:200.000 scale*. Geological Department of Vietnam, Hanoi [Tình H.X. (chủ biên), 2000. *Báo cáo kết quả đo vẽ bản đồ và tìm kiếm khoáng sản tờ Bảo Lạc tỷ lệ 1:200.000*. Lưu trữ Cục địa chất và khoáng sản Việt Nam, Hà Nội].

Tri T.V. & Khuc V. (ed.), 2011. *Geology and Earth Resources of Vietnam*. General Department of Geology and Minerals of Vietnam, Publishing House for Science and Technology, Hanoi.

Ueda A. & Sakai H., 1984. Sulfur isotope study of Quaternary volcanic rocks from the Japanese islands arc. *Geochimica et Cosmochimica Acta*, 48, 1837–1848. https://doi.org/10.1016/0016-7037(84)90037-1.

Ünal-Çakır E., 2020. Sulphur and lead isotope geochemistry of the Dursunbey (Balıkesir) lead-zinc deposit. *Journal of African Earth Sciences*, 172, 104003. https://doi.org/10.1016/j.jafrearsci.2020.104003.

Velasco F., Pesquera A. & Herrero J.M., 1996. Lead isotope study of Zn-Pb ore deposits associated with the Basque-Cantabrian basin and Paleozoic basement, Northern Spain. *Mineralium Deposita*, 31, 84–92. https://doi.org/10.1007/BF00225398.

White W., 1998. *Isotope Geochemistry*. Geological Sciences Course, 656, Earth & Atmosphere Science Department, Cornell University, UK.

Xue C., Zeng R., Liu S., Chi G., Qing H., Chen Y., Yang J. & Wang D., 2007. Geologic, fluid inclusion and isotopic characteristics of the Jinding Zn-Pb deposit, western Yunnan, South China: A review. *Ore Geology Reviews*, 31, 337–359. https://doi.org/10.1016/j.oregeorev.2005.04.007.

Xuyen T. (ed.), 2000. *Report on results of geological mapping and mineral investigation of Ma Quang sheet at 1:200.000 scale*. Geological Department of Vietnam, Hanoi [Xuyến T. (chủ biên), 2000. *Báo cáo kết quả đo vẽ bản đồ và tìm kiếm khoáng sản tờ Mã Quang tỷ lệ 1:200.000*. Lưu trữ Cục địa chất và khoáng sản Việt Nam, Hà Nội].

Zartman R.E. & Doe B.R., 1981. Plumbotectonicsb – the model. *Tectonophysics*, 75, 135–162. https://doi.org/10.1016/0040-1951(81)90213-4.

Zartman R.E. & Haines S.M., 1988. The plumbotectonic model for Pb isotopic systematics among major terrestrial reservoirs – a case for bidirectional transport. *Geochimica et Cosmochimica Acta*, 52, 1327–1339. https://doi.org/10.1016/0016-7037(88)90204-9.